Cell Motility and the Cytoskeleton 58:175–185 (2004)

Molecular Dissection of the Fibroblast-Traction Machinery

Ravi K. Sawhney[1,2] and Jonathon Howard[1,3]*

[1]*Max Planck Institute of Molecular Cell Biology and Genetics, Dresden, Germany*
[2]*Molecular and Cellular Biology Program, University of Washington, Seattle*
[3]*Department of Physiology and Biophysics, University of Washington, Seattle*

Motile fibroblasts generate forces that can be expressed as cell migration or as traction, the drawing-in of extracellular matrix. Traction by cultured fibroblasts can induce a rapid concerted reorganization of collagen gel, creating a pattern of collagen alignment similar to that seen in tendons and ligaments. In such fibrous connective tissues, after pattern morphogenesis is complete, ongoing traction may be responsible for the maintenance of proper form and function. The molecules that generate and transmit forces have been catalogued; however, how these nanometer-scale molecules contribute to millimeter-scale patterns has not been directly tested. Here, we placed pairs of explants of human periodontal ligament fibroblasts in collagen gels, where ligament-like straps of anisotropic collagen formed on the axes between them. We scrutinized the traction apparatus using electron microscopy, video microscopy, and computer-based pattern analysis, augmented with pharmacologic inhibitors of cytoskeletal function. Patterning was marked by the co-alignment of collagen, fibroblasts, and their actin cytoskeletons, all parallel to the axis between explants. The pattern was diminished by depolymerizing actin filaments or by blocking myosin activity, but was accentuated by depolymerizing microtubules. The plasma membrane also seems to contribute to the traction force. These molecular components combine to exert a sub-maximal traction force on the matrix, suggesting that the force may be regulated to ensure tissue tensional homeostasis. Cell Motil. Cytoskeleton 58:175–185, 2004.

Key words: traction; anisotropy; contrast; collagen; tensegrity

INTRODUCTION

The fibrous connective tissues impart stability and integrity to the body. For example, tendons and ligaments are able to withstand tremendous repetitive tensile loading. Their high longitudinal stiffness stems from collagen, the major structural component of the extracellular matrix, which is densely packed and aligned parallel to the primary axis of tissue strain. The alignment of collagen fibers is mediated by fibroblasts. These cells generate tensile forces, referred to as "traction forces," which are transmitted via focal contacts to the underlying substrate or surrounding extracellular matrix [Harris et al., 1980; Fray et al., 1998; Beningo et al., 2001]. When contacts are anchored symmetrically and contracted toward the center of the cell, the cell will remain stationary, but the attached matrix will be drawn in. The resulting stress and strain of matrix are collectively termed simply "traction." Experiments by A.K. Harris and D. Stopak showed that, on the axis between two explants of fibro-

The supplemental material referred to in this section can be found at http://www.interscience.wiley.com/jpages/0886-1544/suppmat/index.html

Contract grant sponsor: Max Planck Society; Contract grant sponsor: Craniofacial Research.

*Correspondence to: Jonathon Howard, MPI-CBG, Pfotenhauerstrasse 108, 01307 Dresden, Germany. E-mail: howard@mpi-cbg.de

Received 26 November 2003; Accepted 11 February 2004

Published online in Wiley InterScience (www.interscience.wiley.com).
DOI: 10.1002/cm.20004

blasts embedded millimeters to centimeters apart in a collagen gel, collagen becomes aligned into a ligament-like strap [Harris et al., 1981]. Such patterns were first described by Paul Weiss, in his classic explorations of the two-center effect in plasma clots [Weiss, 1934]. We have previously shown that small movements of cells in collagen induce a global rearrangement of the collagen gel, driven by traction and amplified by the geometry of the collagen mesh [Sawhney and Howard, 2002]. Collagen is drawn centripetally toward the explants, producing a small tensile strain of matrix on the axis between the explants and a large orthogonal movement of collagen in toward the axis, aligning collagen into a dense anisotropic strap. It has been proposed that traction similarly drives the alignment of collagen during morphogenesis and wound healing of fibrous connective tissues [Harris et al., 1981; Stopak and Harris, 1982; Stopak et al., 1985; Sawhney and Howard, 2002].

Ligaments and tendons are longitudinally stiff, yet they are also dynamic. Tissue forces must be regulated in order to maintain a level of tension high enough to resist creep induced by muscle tone and to stabilize joints between bones [Tkaczuk, 1968; Levine, 1982], yet not so high as to result in pathological contracture. In a culture force monitor, fibroblasts have been shown to regulate their traction forces in a feedback manner, thus providing a potential explanation for the tensional homeostasis seen in mature tissues [Brown et al., 1998]. Furthermore, once patterning of collagen is complete in vitro, killing the cells leads to a partial relaxation of the pattern [Guidry and Grinnell, 1986; Sawhney and Howard, 2002]. This demonstrates that although fusion of aligned collagen fibers may contribute to pattern stability, active fibroblast traction is also important for maintenance of tissue form.

Both cell traction and migration require extension of the leading edge, attachment to substrate, and then contraction [Bray, 2001; Sawhney and Howard, 2002]. Actin polymerization is known to underlie extension [Mitchison and Cramer, 1996; Svitkina et al., 1997; Mullins et al., 1998]. Myosin II drives contraction [Guidry and Grinnell, 1985; Jay et al., 1995; Cramer et al., 1997; Cramer, 1999]. Microtubules modulate attachment and contraction, although their roles in cell motility are controversial [Danowski, 1989; Kolodney and Elson, 1995; Brown et al., 1996; Enomoto, 1996; Kaverina et al., 1999; Wang et al., 2001]. Dynamic focal adhesions have been shown recently linking the cytoskeleton to the collagen matrix, allowing transmission of traction forces to the immediate vicinity of the motile fibroblasts [Petroll et al., 2003; Petroll and Ma, 2003].

It is likely that actin, myosin, and microtubules are also involved in long-distance traction patterning of collagen. However, this hypothesis has not been directly tested, possibly because it has been difficult to quantify patterning. We have recently demonstrated a system in which we can simultaneously observe cell activity and accurately measure matrix movements and anisotropy during alignment of collagen gels [Sawhney and Howard, 2002]. Here we apply these techniques, along with electron microscopy, to investigate the determinants of traction patterning.

We show that fibroblasts, their actin cytoskeletons, and collagen all become co-aligned during collagen patterning. In this arrangement, the cells exert a sub-maximal traction force that deforms the gel. The deformation is diminished by inhibiting myosin activity or depolymerizing actin filaments, but is increased by depolymerizing microtubules. The membrane may also contribute to gel tension. Our results complement measurements of cellular force generation in isolated cells cultured on various deformable substrates [Lee et al., 1994; Galbraith and Sheetz, 1999; Balaban et al., 2001; Beningo et al., 2001]. We provide direct visualization of how these forces generated by intracellular molecules translate into the more clinically and developmentally relevant gross movements of matrix and extracellular patterning. These experiments also demonstrate a novel and convenient method of assessing activities of various mechanical components of cells.

MATERIALS AND METHODS

Experimental Setup

Explants of primary human periodontal ligament-fibroblasts were embedded in collagen gels as previously described [Sawhney and Howard, 2002] using a protocol modified from Stopak and Harris [1982]. Acid-solubilized type I collagen (Cohesion Technologies) was neutralized and diluted to 1.5 mg/ml in HEPES-buffered low-glucose DMEM plus penicillin-streptomycin and 10% fetal bovine serum (all reagents from GIBCO BRL, Gaithersburg, MD). This mixture (475 μl)was added to a 35-mm culture dish with a 1.5 coverslip floor (Mattek), and allowed to polymerize overnight at 37°C in normal atmosphere.

The following morning, cells were trypsinized, concentrated by centrifugation, and pipetted onto the surface of the collagen gel to form explants approximately 0.5 mm in diameter. Cells were allowed to settle and attach to the collagen matrix for 1 h at 37°C, after which 525 μl of 1.85 mg/ml collagen mixture was added. In matrix-tracking experiments, 6- to 16-μm-diameter glass spheres (Mo-Sci) were suspended in the second collagen mixture; these settled to the cell level and served as reference points. The dishes were then kept at 37°C. Samples were placed in a humid 37°C chamber (custom-built with parts from Cell MicroControls) on the micro-

scope stage and 1 ml of media was gently pipetted over the top. This layer prevented the gel from being disturbed during subsequent drug addition. After 8 to 10 h of pattern formation, samples were treated with combinations of cytochalasin D, butanedione monoxime (BDM), nocodazole, and deoxycholate (all from Sigma-Aldrich, St. Louis, MO). Drugs were dissolved in pre-warmed media with 10% fetal bovine serum, at concentrations necessary to yield the desired final concentrations when added to the gel. Drug potency was tested by treating cells plated on glass in the presence of fetal bovine serum.

Microscopy

Live-cell images were obtained on a Diaphot 200 inverted microscope (Nikon), using a 10× phase contrast objective, a 0.6× video coupler (Diagnostic Instruments), and a MicroMax-1300Y cooled CCD camera (Princeton Instruments), driven by Metamorph imaging software (Universal Imaging). Images were obtained once per minute, and raw data were stored as uncompressed 8-bit digital tiff files.

Samples to be sectioned were prepared as above, but left in a 37°C incubator for 18 h to allow pattern formation. Samples were fixed in 2% paraformaldehyde, 2.5% EM grade glutaraldehyde, and 0.1M cacodylate buffer pH 7.35 for 4–24 h at 4°C. After thorough washing, samples were post-fixed with 1% OsO_4 in 0.1M cacodylate buffer for 90 min at room temperature. They were then dehydrated to 70% ethanol and stained en bloc with 3% uranyl acetate in 70% ethanol for 1 h in the dark. Dehydration was continued to absolute alcohol, then samples were infiltrated overnight with Spurrs low-viscosity embedding resin and polymerized for 48 h at 70°C. Sections (1 μm) were cut and stained with 1% Toluidine blue in 1% sodium borate. These were imaged in brightfield on an Axiovert 200 with a 40× plan Neofluar oil-immersion objective (Zeiss, Thornwood, NY), with a Spot CCD camera (Diagnostic Instruments) driven by IPLab software.

Ultra-thin (80–100 nm) sections were cut with a diamond knife and mounted on 100 mesh, formvar-coated copper grids. These sections were stained with 1% phosphotungstate, 7% uranyl acetate, then lead citrate, and examined with a JEOL 1200EX II transmission electron microscope at an accelerating voltage of 80 kV.

Image Analysis

Collagen patterning was quantified using a computer-based algorithm described previously [Sawhney and Howard, 2002]. Stacks of sequential images were prepared for analysis using NIH Image software. A region of the strap image, usually 60 × 360 pixels in size, at 1.1 μm per pixel, was imported into Igor Pro (WaveMetrics) for measurement of the anisotropy of image contrast. Briefly, the program dissects the image into a collection of lines, each oriented either parallel or perpendicular to the forming strap. In a mature strap, lines along the axis of alignment tend to be all light or all dark and, therefore, of low contrast (standard deviation over the mean of the pixel values), whereas those perpendicular to the axis tend to be of higher contrast. The relative difference between the average parallel and perpendicular contrasts serves as our anisotropy index.

Redistributions of collagen during patterning were analyzed by tracking glass spheres dispersed in the gel, using NIH Image.

RESULTS

Ultrastructure of the Traction Elements

In order to investigate the molecular components involved in collagen traction-patterning and stabilization, pairs of explants of human periodontal ligament fibroblasts were embedded approximately 1 mm apart in collagen gels. After 18 h, enough time for straps of aligned collagen to form on the axes between explants (see Figs. 2, 3, and 6), samples were fixed, mounted, sectioned, and stained appropriately for either brightfield (Fig. 1a and b) or electron microscopy (Fig. 1c–f). Horizontal sections through the plane of the two explants, situated at the upper left and lower right, revealed three zones of collagen architecture: an alignment zone, a compaction zone, and a transition zone in between (Fig. 1a and b). In the alignment zone or strap, long straight collagen fibers remain in the plane of section for over 100 μm, and are aligned parallel to the axis between the explants. The aligned fibers often radiate from cell processes extending from one to the opposing explant. Although a background of randomly oriented fibers persists, the aligned fibers are consistent with the dramatic strap pattern seen in phase contrast of live tissues (Figs. 2, 3; see also Fig. 6). Within the explant is a zone of compaction where cells are polyhedral, rather than elongated, and dense collagen fills the spaces between cells. Because strap formation involves little net movement of collagen along the axis between explants [Sawhney and Howard, 2002], the compacted collagen was likely traction-drawn from regions above, below, and lateral to the explants. In between the alignment and compaction zones, is the transition zone populated with elongated fibroblasts extending from the explant. Fibroblasts were rarely seen detached from the explants, but rather maintained connection through neighboring cells. In this transition zone, collagen was neither compacted nor aligned. The lack of alignment suggests that in this zone, the tension causing strap alignment is transmitted by the

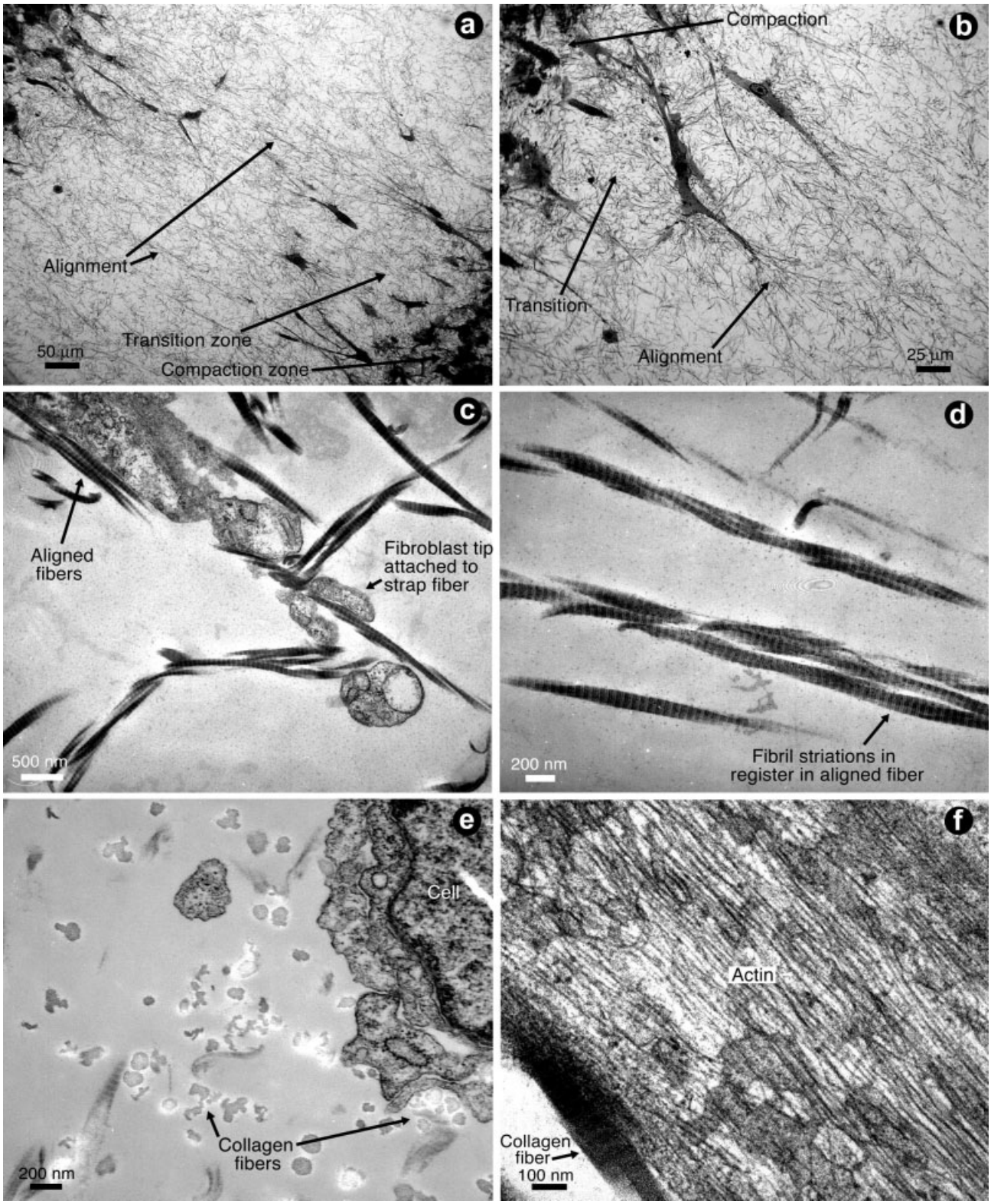
a
Alignment
Transition zone
Compaction zone
50 μm
b
Compaction
Transition
Alignment
25 μm
c
Aligned fibers
Fibroblast tip attached to strap fiber
500 nm
d
Fibril striations in register in aligned fiber
200 nm
e
Cell
Collagen fibers
200 nm
f
Actin
Collagen fiber
100 nm

Figure 1.

cells rather than across the collagen. This demonstrates that these fibroblasts are exerting a traction force.

Electron microscopy was used to explore the subcellular source of the traction force in the transition zone (Fig. 1c, d, and f are all in roughly the same orientation as a). Collagen fibers project from fibroblast processes extending toward the opposing explant (Fig. 1c). Fibers often appear to be contiguous with a cell process, either along the lateral boundary of the process, or enveloped by its anterior tip. Tracking along such fibers on the axis between explants shows that fibers parallel to the axis predominate in the strap-patterned region (Fig. 1d). The characteristic 67-nm periodic striations of type I collagen fibrils are visible. These striations are in register in adjacent fibrils within a given fiber, indicating that the fibrils have fused. In a section cut perpendicular to the explant-explant axis (Fig. 1e, same magnification as d), the fibers have irregular cross-sections and varying diameters. Again, fibers are often seen close and potentially attached to the cell process. In the soma of the cell from Figure 1c, actin filaments of the cytoskeleton are densely packed and aligned parallel to the attached collagen fiber seen in the lower left (Fig. 1f).

It is impossible to determine from our experiments the forces and effects of the fibroblasts that reside within the compaction zone, toward the center of the explants. However, from the views of collagen and cells in the transition zone (Fig. 1a–c,f), it does seem that the transition zone fibroblasts are active in the process of traction patterning. There, the irregular fiber orientation suggests that transition zone fibers are not bearing load, whereas the alignment of fibroblasts and their actin cytoskeletons parallel to the collagen fibers of the strap suggests that these cells are bearing load. Thus, the cells at the periphery of the explant are poised to exert traction forces that draw collagen into close alignment, where they can possibly fuse and stabilize the strap pattern [Sawhney and Howard, 2002].

Fig. 1. Collagen, cells, and their cytoskeletons all align during 18 h of strap patterning. Brightfield images of fixed, toluidine-stained gels. **a:** A horizontal section through the strap with the edges of explants in the top left and bottom right corners. (Except e, all panels are in a similar orientation.) Fibroblast traction has led to the formation of three zones of matrix architecture. In the alignment zone, fibers remaining in the plane of section for hundreds of microns, parallel to the axis between the explant, emanate from extended fibroblasts, but randomly oriented fibers persist. In the compaction zone, cells are polyhedral instead of elongated and collagen is dense in the interstices. Between the areas of alignment and compaction is a transition zone, populated by extended fibroblasts, where collagen is neither compacted nor aligned. **b:** Higher magnification of fibroblasts at the edge of an explant, aligned parallel to the strap. The three zones are apparent. Transmission electron micrographs: **c:** The anterior process of an extended cell of the transition zone with aligned fibers along its surface; the tip envelops a collagen fiber extending into the strap. **d:** Aligned collagen fibers of the alignment zone are comprised of intertwined collagen fibrils, with their characteristic 67-nm banding patterns in register. **e:** At the same magnification as, but perpendicular to the strap, the cell is in the top right, and collagen fibers are in the center of the image. Banded ribbons are fibers traversing the section at intermediate angles relative to the plane. The majority of fibers are in cross-section, are seen to be of irregular shapes and sizes, and often are in close proximity to the cell. **f:** In the body of the cell whose tip is shown in c, the actin lattice is densely packed, parallel to the axis of strain and to the collagen fiber seen in the bottom left.

Inhibition of Actin and Myosin Diminishes the Traction Pattern

In order to more directly explore the roles of various cell components in traction, patterned gels were treated with cytoskeleton inhibitors. Two explants were embedded in a collagen gel, incubated for 7 h to allow strap formation, then placed in the microscopy chamber. Glass spheres had been dispersed in the gel where they remained stationary relative to local collagen architecture and, therefore, served as reference points for tracking cell and matrix movements. Initially (Fig. 2a), fibroblasts displayed long prominent processes, extending radially from the explant surfaces. The processes had branching tips or fan-shaped lamellae at their leading edges. A strap of aligned collagen had already formed. Positions of beads that were tracked are shown. After 1 h of filming, cell morphology had not changed (Fig. 2b). At that time, 5 μM cytochalasin D was added to depolymerize actin filaments. The positions of beads immediately before (orange) and after (yellow) showed that the gel was not disturbed during pipetting. After 1 h of drug treatment, the explants had expanded perpendicular to the axis between explants, although general explant morphology was similar. Cytochalasin D treatment led to a loss of branching and a blunting of cell processes, but the strap persisted (Fig. 2c). Then, at hour 9, deoxycholate was added without disturbing the gel (compare bead positions: yellow before vs. red after). Cells quickly blurred into the surrounding matrix as cell membranes were destroyed. After an hour (Fig. 2d), only a dark halo remained where the explants were, but the aligned strap was still visible. Figure 2d shows bead tracking data for the entire experiment. Bead paths throughout the experiment are displayed at 10-min intervals, with arrows added to depict directions of movement at various stages (in this and all drug experiments: orange = initial movements without intervention, yellow = movements in the presence of drug, and red = movements after addition of deoxycholate detergent). During the first hour, bead movements indicated that the strap was still forming: beads on the strap axis moved slightly toward the explants and beads in adjacent regions moved laterally toward the axis. After addition of cytochalasin D, their paths reversed, moving rapidly at first (5.6 ± 1.7 μm/min

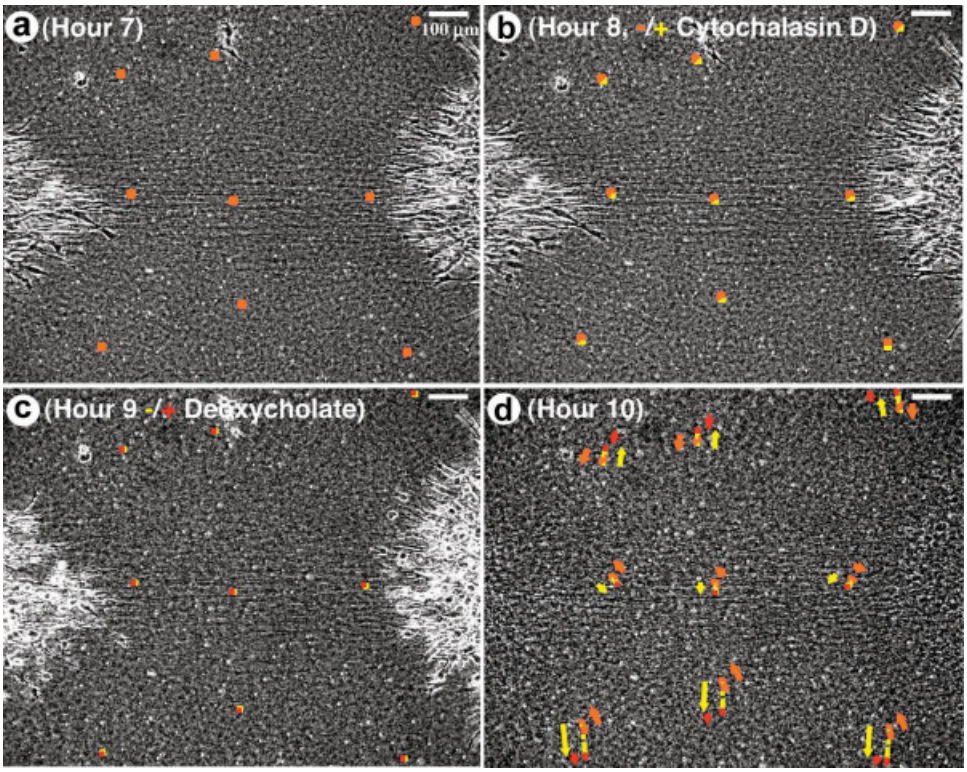

Fig. 2. Depolymerization of actin causes strap relaxation. At hour 0, two explants were embedded in collagen with dispersed glass beads. **a:** By hour 7, fibroblast traction had aligned collagen into a strap. **b:** After 1 h of filming, cytochalasin D was added to 5 μM. Positions of selected beads immediately before (*orange*) and after (*yellow*) drug addition demonstrate that gel was not disturbed. **c:** After an hour of cytochalasin D treatment, the explants had expanded perpendicular to the strap. At this point, deoxycholate was added with no gel shift (yellow before vs. red after). **d:** Cells burst within 10 min. Tracks of beads are shown at 10-min intervals, with *arrows* added to depict direction of movement; *orange*, the initial movement showing that the strap was still slowly forming; *yellow*, with cytochalasin, movement reversed as pattern partially relaxed; *red*, with addition of detergent, there was a small continuation of the relaxation, evident in a timelapse video (Fig. 2 Video). Some residual collagen alignment remained at Hour 10.

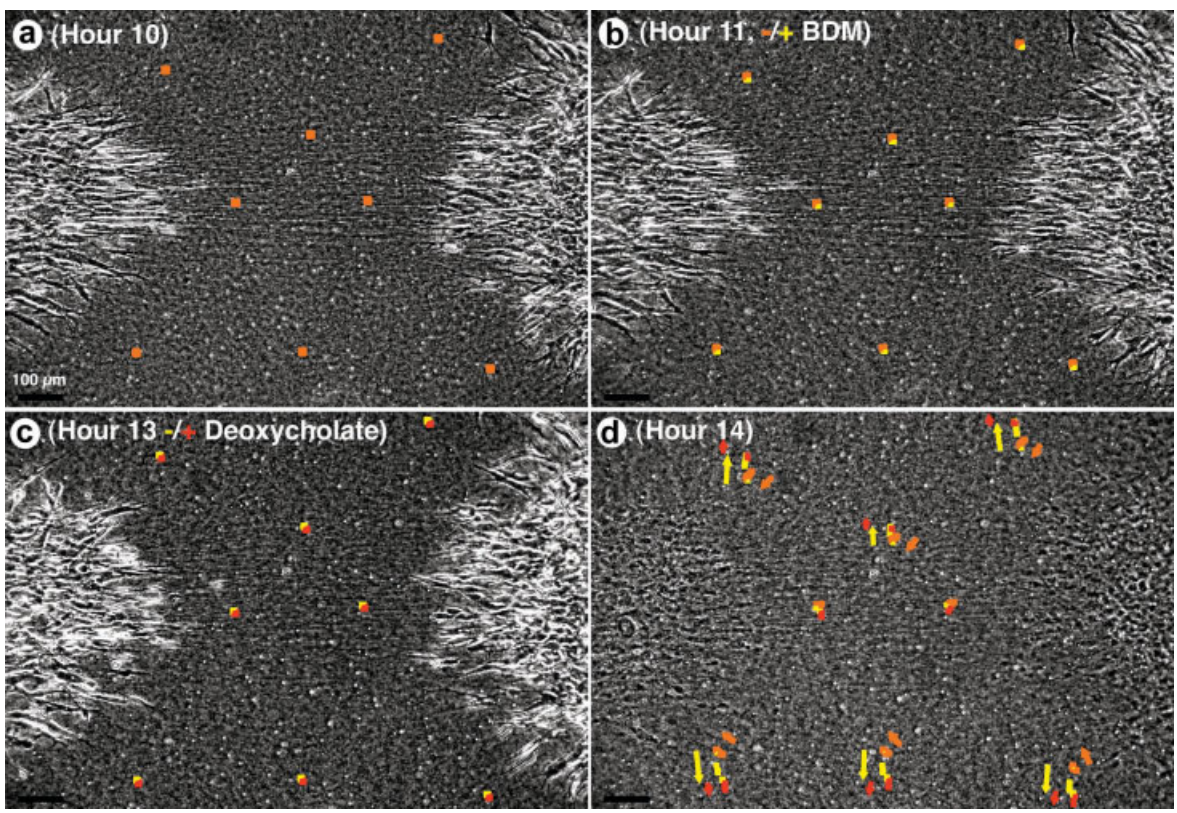

Fig. 3. Inhibition of myosin causes strap relaxation. **a:** After 10 h, the strap was already formed. Filming commenced to establish baseline movements. **b:** After 1 h, cells looked the same; BDM was added to 30 mM. **c:** After an hour of BDM treatment, deoxycholate was added. **d:** After 1 more hour, cells were dead. Tracks of beads are shown at 10-min intervals; *orange*, initial movement shows strap was still slowly forming; *yellow*, with BDM, matrix movement reversed indicating a decrease in the traction force. With addition of detergent, there is a small continuation of the relaxation, evident in a timelapse video (Fig. 3 Video). A remnant of the aligned strap remained at Hour 14.

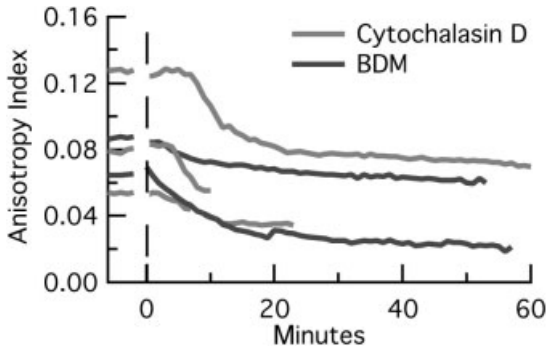

Fig. 4. Cytochalasin D and BDM cause relaxation of pattern. In five experiments, drug was added at time = 0 min. Contrast analysis shows that in all experiments, anisotropy declines and levels off within 30 min, but does not reach zero.

for 6 tracked beads adjacent to the strap), then slowing to a halt near the end of the hour. As seen in previous experiments [Sawhney and Howard, 2002], pattern release was marked by a lateral movement of matrix, perpendicular to and away from the strap. Deoxycholate induced a slight further relaxation of the strap, also evident in timelapse video (Fig. 2, Video).

A similar experiment was done using BDM, a drug with multiple activities, most commonly used as an inhibitor of myosin (See Discussion). The strap was allowed to form during the 10 h prior to filming. At that time, cells exhibited long branching processes radiating away from the explants (Fig. 3a). After 1 h, 30 mM BDM was added to the culture without disturbing the gel (Fig. 3b). BDM induced a partial relaxation of the strap, with beads moving nearly perpendicular to and away from the axis between explants. After 2 h of BDM treatment, deoxycholate was added to kill the cells (Fig. 3c). This detergent induced a small further release of strap pattern (more obvious in time-lapse; see Fig. 3, Video). However, residual strap alignment remained clearly visible after 1 h (Fig. 3d). Tracking data indicated that, again, small movements were occurring at the onset of the experiment, consistent with strap formation.

The release of strain within the collagen matrix induced by cytochalasin D and BDM was accompanied by a diminution of the strap pattern (Fig. 4). Contrast analysis (see Materials and Methods) demonstrated that inhibition of the actin-myosin machinery led to a decrease in gel anisotropy by almost half (42 ± 15% reduction, $n = 5$) nearly completed after 20 min.

To correlate the effect of the drugs on the strap with changes in cell morphology, we tested the potency and time course of action of the actin and myosin inhibitors on fibroblasts adhering to glass, where changes in cell morphology could be seen in greater detail. Initially, cells had typical bi- or tri-polar forms with well-spread lamellae (Fig. 5a and c). After addition of 5 μM cytochalasin D, cells rapidly collapsed as broad ruffling lamellae narrowed into strings that were pulled toward the cell

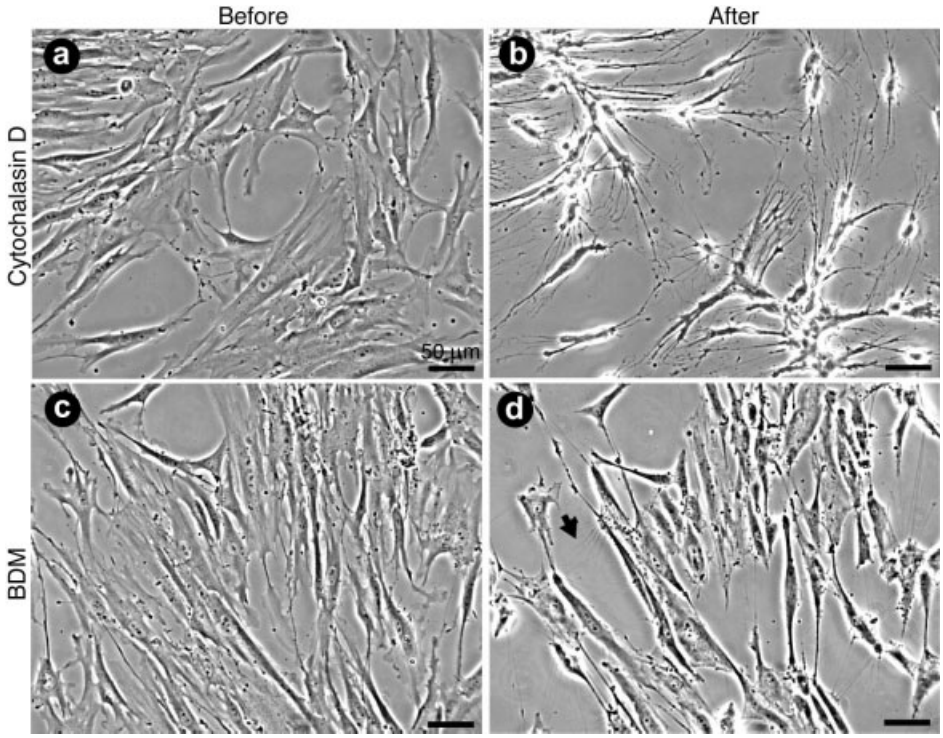

Fig. 5. Effects of cytochalasin D and BDM on fibroblasts on glass. Before treatment (**a** and **c**), cells displayed normal bipolar shapes with ruffling borders (Fig. 5B and 5D Videos). **b:** After 20 min in the presence of 5 μM cytochalasin D, cell borders had retracted significantly, and tracks of cell debris remain. **d:** After 75 min with 30 mM BDM, retracting lamellae have left behind fine hair-like processes (*arrow*). Relative movements of hairs and cells in time-lapse reveal that the hairs were not microspikes projecting from cells, but rather represent unreleased attachments to glass and other cells.

center, leaving tracks of debris behind them (Fig. 5b, Fig. 5b Video). Over the course of an hour, sheets of cells were drawn into clumps, and individual cells into balls.

The effects of 30 mM BDM on cells on glass were more subtle. After 75 min (Fig. 5d), fibroblasts were still elongated, and partially spread, but had hair-like strands emanating from their surfaces. Time-lapse recordings showed that ruffling activity stopped immediately upon addition of BDM, and lamellae began to slowly retract (Fig. 5d Video). As cells retreated, they left behind finger-like projections, which were further drawn into the fine processes extending roughly perpendicular to their surfaces, as seen in Figure 5d. Judging from their angles of movement with respect to the retreating cells, some of these processes were attached to glass substrate, and others to other cells.

These experiments demonstrated that 75 min of treatment with either 5 μM cytochalasin D or 30 mM BDM has a profound effect on actin-myosin activity and cell morphology. In two further experiments (not shown), single explants of mouse neonatal skin fibroblasts were embedded in collagen, allowed to draw in collagen for 8 h, and then treated with a combination of both 10 μM cytochalasin D and 30 mM BDM for 2 h. Collagen relaxed centrifugally with actin-myosin inhibition, rapidly at first and slowing to almost a halt by the end of the second hour, when cells were killed with detergent. Bead tracking revealed that even with such stringent drug treatment, detergent addition produced an acceleration in the movement of matrix, resulting in a small (~10%) further relaxation of matrix strain.

Depolymerization of Microtubules Accentuates the Traction Pattern

In order to assess the involvement of microtubules in traction-generation, patterned gels were treated with nocodazole (Fig. 6). After 13 h, a strap of aligned collagen had formed and cells were elongated with branched processes extending radially from the explants (Fig. 6a). The sample was filmed for 1 h to confirm baseline stability (Fig. 6b), then nocodazole was added to a final concentration of 10 μM. Bead tracking data for the entire experiment are displayed in Figure 6c. Matrix was stationary for the first hour, indicating that the strap formation was complete by hour 13. Nocodazole induced an increase of matrix distortion, with matrix movements occurring in the opposite direction compared to those seen with cytochalasin and BDM. The effect was confirmed in another bead tracking experiment. In both, the increased traction was more obvious in time-lapse video (Fig. 6 Video), where explants could be seen contracting, drawing nearby collagen centripetally toward the explants and, from more distant areas, in toward the explant-explant axis.

To confirm the effect of nocodazole seen in tracking experiments, five experiments were subjected to contrast analysis (Fig. 6D). In all five, addition of nocodazole induced a rise in the anisotropy index, demonstrating that depolymerization of microtubules does lead to an increase in matrix traction.

DISCUSSION

The molecular basis of traction

We have combined direct visualization of matrix patterning with drugs that disturb various aspects of cell function in order to identify the cellular components involved in generating and modulating the traction force and pattern. Ultrastructural analysis of collagen gels revealed that patterning involves a coalignment of collagen fibers, fibroblasts, and their actin cytoskeletons, all lining up parallel to the axis between two explants (Fig. 1). As expected, actin and myosin provided the primary source of the traction force. Actin depolymerization led to a decrease in traction (Figs. 2 and 4) and to a decrease in extension or ruffling activity (Fig. 5 and Fig. 5b Video). BDM treatment led to a similar decrease in traction (Figs. 3 and 4), presumably due to inhibition of myosin. These results should be interpreted with care in light of recent reports describing non-specific effects of BDM [Waterman-Storer, 1997; Turvey et al., 2003], and a lack of effect on some myosins [Ostap, 2002]. BDM is, however, widely accepted as an effective inhibitor of some isoforms of myosin II [Cramer and Mitchison, 1995; Ostap, 2002], a major determinant of cell shape and movement. With those caveats in mind, we will assume for discussion here that the primary mechanism of BDM's effect on cell morphology and traction is its inhibition of myosin function.

Unexpectedly, loss of myosin—normally associated with tension generation—led to retraction of the cell edges. However, both in collagen and on glass, cells remained attached to the substrate and to neighboring cells (Figs. 3 and 5d). This result was in contrast to a report suggesting that inhibition of myosin leads to edge retraction secondary to dissociation of peripheral substrate contact sites [Kaverina et al., 1999]. The retraction in the presence of contacts suggests that in addition to its motor function, myosin may serve as a more generic actin-crosslinking agent to promote the integrity (as opposed to the tensegrity) of the actin skeleton. It could act similarly to α-actinin, producing a cortex that is rigid when challenged by rapid forces, but susceptible to deformation by forces of long duration [Sato et al., 1987]. These issues deserve further exploration through biophysical techniques and fluorescence microscopy, augmented with emerging inhibitors with improved specificity.

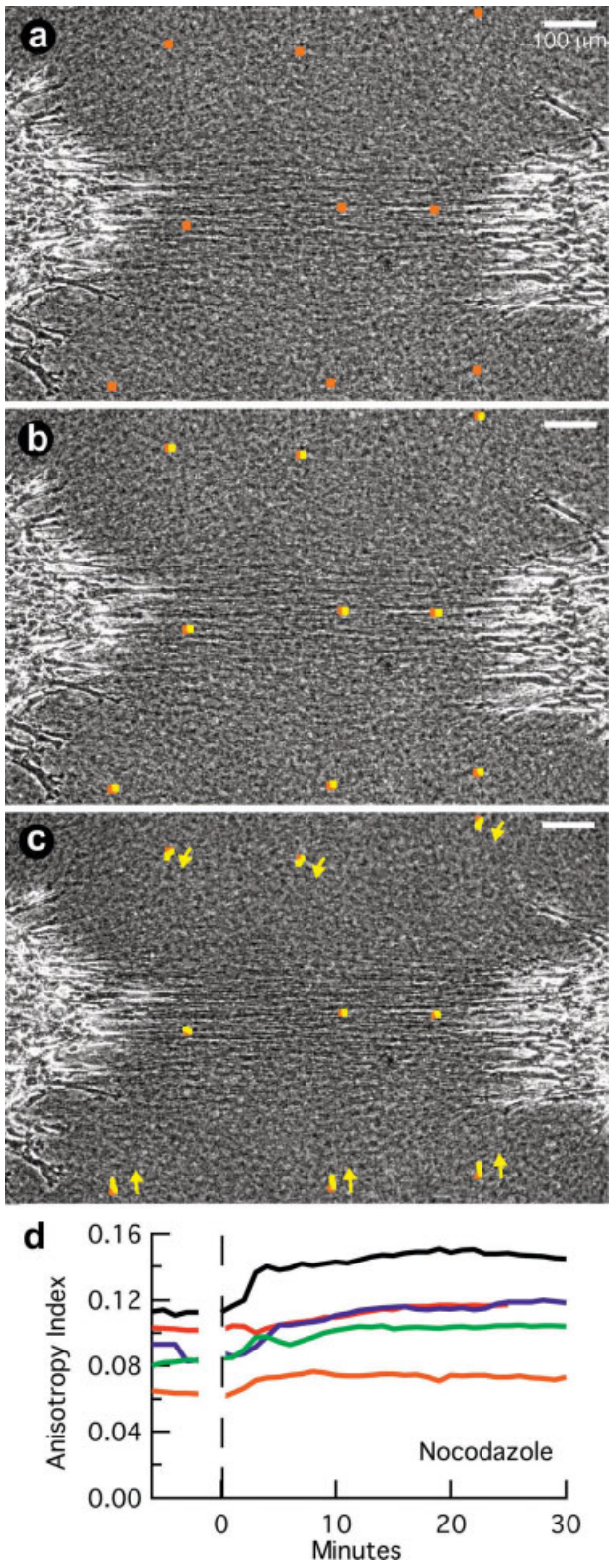

The collapse of cells accompanying the loss of the myosin-derived cytoskeletal integrity in our experiments (Fig. 5d) suggests that membrane-tension may be important in the determination of cell-shape. Membrane tension is often ignored in analyses of cell morphology. Although valuable for observation of fine structures, experiments using glass substrates are compromised by the fact that cells perform differently on deformable substrates, or in more-physiologic three-dimensional matrices. So, further evidence for a possible mechanical role of the membrane was the finding that detergent treatment, after stringent inhibition of the actin-myosin system, led to a relaxation of the collagen pattern (Figs. 2, 3, and single-explant experiments not shown). It could be argued that the detergent is breaking some crosslinks in the collagen matrix and leading to further relaxation, or that there are drug-resistant populations of actin and myosin that continue to exert a traction force until cell death. However, the fact that the cell membranes do remain tethered to substrate even with extended drug treatment (Figs. 2c, 3c, 5b,d) and that the tethers are destroyed with membrane solubilization, it seems more likely that the further release of strain associated with detergent addition is due to the loss of tensile force derived from the membrane itself.

Microtubule depolymerization increased the traction distortion of matrix (Fig. 6). The mechanism underlying this effect is debatable. At the heart of the controversy are two competing classes of models for the governance of cell shape. We term these the global-pull and the local-push models. In the global-pull theories, cell shape is governed at the level of the entire cell and tends to be dictated by the activity of tensile elements. Examples include toothpaste-tube models for protrusion [Stossel et al., 1999] and the tensegrity model [Fuller, 1961; Levine, 1982], in which the cell functions as an integrated unit, with actomyosin filaments serving as the active tensile elements, microtubules forming compressive struts, and intermediate filaments reinforcing the lattice by working as guy wires to prevent microtubule buckling [Ingber, 1993]. In such an arrangement, depolymerization of microtubules would cause a collapse of the cell, thus transferring the load from microtubules to the surrounding matrix [Brown et al., 1996]. However, all traction studies demonstrate that tensile forces in cells

Fig. 6. Depolymerization of microtubules causes an increase in traction. **a:** Strap formed over 13 h before filming began. **b:** After 1 h, 10 µM nocodazole was added. **c:** Trackings: *orange*, no movement occurred between hours 13 and 14; *yellow*, with addition of nocodazole, there was an increase in compression of matrix and explants toward the axis of traction. Arrows indicate directions of movement. **d:** In five experiments, nocodazole addition at time 0 effected an increase in strap anisotropy within 20 min.

are at least partially borne by the substrate, proving that cell shape is not defined solely by tensegrity elements, but also by attachments to surrounding matrix. This does not, however, rule out a more limited role for tensegrity or global-pull principles.

In contrast, in the local-push models, functional units of extension are more localized, and compressive elements dominate. A classic example of a local-push theory model is that from Oster [1984], in which a local increase in osmotic pressure drives cell protrusion. The most commonly accepted local-push model is the "treadmilling dendritic brush" [Svitkina et al., 1997], or "dendritic nucleation" model [Mullins et al., 1998] in which a polymerizing actin array in the cell lamella drives the leading edge forward. The array is anchored to the substrate through focal contacts [Anderson and Cross, 2000] and is thus stationary with respect to the substrate [Verkhovsky et al., 1999]. Elongating actin filaments are compressed between focal contacts and the leading edge, extending the cell by applying a rearward force to the underlying substrate [Galbraith and Sheetz, 1999], rather than to the rest of the cell. Discrimination between the global-pull and local-push models is confused by the fact that depolymerization of microtubules is thought to cause a loss of kinesin-based delivery of a Rho-inhibitor, thereby diminishing stress fibers and their associated contacts [Enomoto, 1996; Kaverina et al., 1999], and also to a loss of microtubule-dependent activating phosphorylation of the myosin regulatory light chain [Kolodney and Elson, 1995]. It is possible that the accentuation of the traction-pattern brought about by nocodazole in our experiments was due either to blockage of such intracellular transport functions of microtubules or to their mechanical properties; however, the effect may well be a consequence of a combination of the two.

Regardless, the fact that microtubule depolymerization boosts the traction force demonstrates that fibroblasts in patterned gels are exerting a sub-maximal force, which they may potentially regulate. Brown and coworkers have shown that populations of cells in collagen matrix can modulate their traction forces in response to mechanical signals in order to maintain tensional homeostasis [Brown et al., 1998]. Unfortunately, in their culture force monitor, it was impossible to simultaneously visualize cell changes and measure forces. With modifications, our system may provide an ideal venue for testing hypotheses involving global-pull and local-push models of cell-shape determination, as well as the mechanical control of development and maintenance of tissue form.

Clinical Implications of Traction Patterning

The alignment of cells and collagen during patterning leaves the cells poised to maintain and regulate appropriate tension in the matrix, an arrangement that may mimic the form and function of the dense fibrous connective tissues. For example, in skin ongoing traction could lead to tone or to the maintenance of integrity during aging. Another example is the periodontal ligament that supports a tooth in its bony socket like a sling, with fibroblasts interspersed amongst fibers coursing from high on the bone to low on the tooth root [Beertsen et al., 1997]. In this orientation, traction forces generated by fibroblasts could maintain collagen alignment in order to best resist loading during chewing. The strain-rate sensitivity imparted by myosin cross-linking activity may help to explain why teeth are not moved by short-duration heavy biting forces, but will move in response to a long duration albeit gentle force exerted by orthodontic appliances ("braces"). Furthermore, due to the orientation of fibers and cells, traction would lead to an upward direction of tooth movement, as is seen during initial emergence into the mouth, or when a tooth is shortened by bruxism (grinding), or when it loses its opponent in the opposing arch.

CONCLUSIONS

For decades, biomedical researchers have been struggling to grasp how actions of small molecules can drive the formation and maintenance of a human body pattern, nine orders of magnitude larger. The complexity and importance of the issue demands a multi-faceted approach, using a variety of tools and techniques for analysis. We have applied a recently developed system for video microscopy and computer-based anisotropy analysis, combined with pharmacologic inhibitors of the cytoskeleton and electron micrography in order to investigate the molecules involved in fibroblast-traction collagen patterning. Our results have provided novel insights into the cellular components of force generation and demonstrate how the system may be useful in further exploration of molecular-mechanical patterning.

ACKNOWLEDGMENTS

We thank Dr. Kurt Anderson for technical help, Ms. Anja Glenk for production assistance, and the Max Planck Society (J.H.) and the National Institute of Dental and Craniofacial Research (R.S.) for financial support.

REFERENCES

Anderson KI, Cross R. 2000. Contact dynamics during keratocyte motility. Curr Biol 10:253–260.

Balaban NQ, Schwarz US, Riveline D, Goichberg P, Tzur G, Sabanay I, Mahalu D, Safran S, Bershadsky A, Addadi L, Geiger B. 2001. Force and focal adhesion assembly: a close relationship studied using elastic micropatterned substrates. Nat Cell Biol 3:466–472.

Beertsen W, McCulloch CA, Sodek J. 1997. The periodontal ligament: a unique, multifunctional connective tissue. Periodontol 2000, 13:20–40.

Beningo KA, Dembo M, Kaverina I, Small JV, Wang YL. 2001. Nascent focal adhesions are responsible for the generation of strong propulsive forces in migrating fibroblasts. J Cell Biol 153:881–888.

Bray D. 2001. Cell movements: from molecules to motility. New York: Garland Pub. 372 p.

Brown RA, Talas G, Porter RA, McGrouther DA, Eastwood M. 1996. Balanced mechanical forces and microtubule contribution to fibroblast contraction. J Cell Physiol 169:439–447.

Brown RA, Prajapati R, McGrouther DA, Yannas IV, Eastwood M. 1998. Tensional homeostasis in dermal fibroblasts: mechanical responses to mechanical loading in three-dimensional substrates. J Cell Physiol 175:323–332.

Cramer LP. 1999. Organization and polarity of actin filament networks in cells: implications for the mechanism of myosin-based cell motility. Biochem Soc Symp 65:173–205.

Cramer LP, Mitchison TJ. 1995. Myosin is involved in postmitotic cell spreading. J Cell Biol 131:179–189.

Cramer LP, Siebert M, Mitchison TJ. 1997. Identification of novel graded polarity actin filament bundles in locomoting heart fibroblasts: implications for the generation of motile force. J Cell Biol 136:1287–1305.

Danowski BA. 1989. Fibroblast contractility and actin organization are stimulated by microtubule inhibitors. J Cell Sci 93:255–266.

Enomoto T. 1996. Microtubule disruption induces the formation of actin stress fibers and focal adhesions in cultured cells: possible involvement of the rho signal cascade. Cell Struct Funct 21: 317–326.

Fray TR, Molloy JE, Armitage MP, Sparrow JC. 1998. Quantification of single human dermal fibroblast contraction. Tissue Eng 4:281–291.

Fuller B. 1961. Tensegrity. Portfolio Arnews Annu 4:112–127.

Galbraith CG, Sheetz MP. 1999. Keratocytes pull with similar forces on their dorsal and ventral surfaces. J Cell Biol 147:1313–1324.

Guidry C, Grinnell F. 1985. Studies on the mechanism of hydrated collagen gel reorganization by human skin fibroblasts. J Cell Sci 79:67–81.

Guidry C, Grinnell F. 1986. Contraction of hydrated collagen gels by fibroblasts: evidence for two mechanisms by which collagen fibrils are stabilized. Coll Relat Res 6:515–529.

Harris AK, Wild P, Stopak D. 1980. Silicone rubber substrata: a new wrinkle in the study of cell locomotion. Science 208:177–179.

Harris AK, Stopak D, Wild P. 1981. Fibroblast traction as a mechanism for collagen morphogenesis. Nature 290:249–251.

Ingber DE. 1993. Cellular tensegrity: defining new rules of biological design that govern the cytoskeleton. J Cell Sci 104:613–627.

Jay PY, Pham PA, Wong SA, Elson EL. 1995. A mechanical function of myosin II in cell motility. J Cell Sci 108:387–393.

Kaverina I, Krylyshkina O, Small JV. 1999. Microtubule targeting of substrate contacts promotes their relaxation and dissociation. J Cell Biol 146:1033–1044.

Kolodney MS, Elson EL. 1995. Contraction due to microtubule disruption is associated with increased phosphorylation of myosin regulatory light chain. Proc Natl Acad Sci USA 92:10252–10256.

Lee J, Leonard M, Oliver T, Ishihara A, Jacobson K. 1994. Traction forces generated by locomoting keratocytes. J Cell Biol 127: 1957–1964.

Levine S. 1982. Continuous tension, discontinuous compression a model for biomechanical support of the body. Bull Struct Integr 8:31–33.

Mitchison TJ, Cramer LP. 1996. Actin-based cell motility and cell locomotion. Cell 84:371–379.

Mullins RD, Heuser JA, Pollard TD. 1998. The interaction of Arp2/3 complex with actin: nucleation, high affinity pointed end capping, and formation of branching networks of filaments. Proc Natl Acad Sci USA 95:6181–6186.

Ostap EM. 2002. 2,3-Butanedione monoxime (BDM) as a myosin inhibitor. J Muscle Res Cell Mot 23:305–308.

Oster GF. 1984. On the crawling of cells. J Embryol Exp Morphol 83(Suppl):329–64.

Petroll WM, Ma L. 2003. Direct, dynamic assessment of cell-matrix interactions inside fibrillar collagen lattices. Cell Motil Cytoskeleton 55:254–264.

Petroll W, Ma L, Jester J. 2003. Direct correlation of collagen matrix deformation with focal adhesion dynamics in living corneal fibroblasts. J Cell Sci 116:1481–1491.

Sato M, Schwarz WH, Pollard TD. 1987. Dependence of the mechanical properties of actin/alpha-actinin gels on deformation rate. Nature 325:828–830.

Sawhney RK, Howard J. 2002. Slow local movements of collagen fibers by fibroblasts drive the rapid global self-organization of collagen gels. J Cell Biol 157:1083–1092.

Stopak D, Harris AK. 1982. Connective tissue morphogenesis by fibroblast traction. I. Tissue culture observations. Dev Biol 90:383–398.

Stopak D, Wessells NK, Harris AK. 1985. Morphogenetic rearrangement of injected collagen in developing chicken limb buds. Proc Natl Acad Sci USA 82:2804–2808.

Stossel TP, Hartwig JH, Janmey PA, Kwiatkowski DJ. 1999. Cell crawling two decades after Abercrombie. Biochem Soc Symp 65:267–80.

Svitkina TM, Verkhovsky AB, McQuade KM, Borisy GG. 1997. Analysis of the actin-myosin II system in fish epidermal keratocytes: mechanism of cell body translocation. J Cell Biol 139:397–415.

Tkaczuk H. 1968. Tensile properties of human lumbar longitudinal ligaments. Acta Orthop Scand Suppl(115):1–69.

Turvey MR, Laude AJ, Ives EOH, Seager WH, CTaylor CW, Thorn P. 2003. Modulation of IP3-sensitive Ca2+ release by 2,3-butanedione monoxime. Pflugers Arch Eur J Physiol 445:614–621.

Verkhovsky AB, Svitkina TM, Borisy GG. 1999. Self-polarization and directional motility of cytoplasm. Curr Biol 9:11–20.

Wang N, Naruse K, Stamenovic D, Fredberg JJ, Mijailovich SM, Tolic-Norrelykke IM, Polte T, Mannix R, Ingber DE. 2001. Mechanical behavior in living cells consistent with the tensegrity model. Proc Natl Acad Sci USA 98:7765–7770.

Waterman-Storer CM SE. 1997. Actomyosin-based retrograde flow of microtubules in the lamella of migrating epithelial cells influences microtubule dynamic instability and turnover and is associated with microtubule breakage and treadmilling. J Cell Biol 139:417–434.

Weiss P. 1934. In vitro experiments on the factors determining the course of the outgrowing nerve fiber. J Exp Zool 68:393–448.